Chemiluminescence lateral flow immunoassay cartridge with integrated amorphous silicon photosensors array for human serum albumin detection in urine samples

Chemiluminescence lateral flow immunoassay cartridge with integrated amorphous silicon photosensors array for human serum albumin detection in urine samples

Martina Zangheri[1], Fabio Di Nardo[2], Mara Mirasoli[1,3*], Laura Anfossi[2], Augusto Nascetti[4], Domenico Caputo[5], Giampiero De Cesare[5], Massimo Guardigli[1], Claudio Baggiani[2], Aldo Roda[1,3]

1 Department of Chemistry “Giacomo Ciamician”, Alma Mater Studiorum - University of Bologna, via Selmi 2, 40126 Bologna, Italy

2 Department of Chemistry, University of Turin, Via P. Giuria, 5, 10125 Torino, Italy

3 Interuniversity Consortium INBB - Viale delle Medaglie d’Oro, 305, 00136 Roma

4 Aerospace Engineering School, Sapienza University of Rome, via Salaria 851/881, 00138, Rome, Italy

5 Department of Information, Electronics and Communication Engineering, Sapienza University of Rome, via Eudossiana, 18 00184, Rome, Italy

* Corresponding Author:

Mara Mirasoli

Department of Chemistry “Giacomo Ciamician”

Alma Mater Studiorum - University of Bologna

via Selmi 2, 40126 Bologna, Italy

mara.mirasoli@unibo.it

Abstract

A novel and disposable cartridge for chemiluminescent (CL)-lateral flow immunoassay (LFIA) with integrated amorphous silicon (a-Si:H) photosensors array was developed and applied to quantitatively detect human serum albumin (HSA) in urine samples. The presented analytical method is based on an indirect competitive immunoassay using horseradish peroxidase (HRP) as a tracer, which is detected by adding the luminol/enhancer/hydrogen peroxide CL cocktail. The system comprises an array of a-Si:H photosensors deposited on a glass substrate, on which a PDMS cartridge, that houses the LFIA strip and the reagents necessary for the CL immunoassay, was optically coupled to obtain an integrated analytical device controlled by a portable read-out electronics.

The method is simple and fast with a detection limit of 2.5 mg L^{-1} for HSA in urine and a dynamic range up to 850 mg L^{-1}, which is suitable for measuring physiological levels of HSA in urine samples and their variation in different diseases (micro- and macroalbuminuria).

The use of CL detection allowed accurate and objective analyte quantification in a dynamic range that extends from femtomoles to picomoles. The analytical performances of this integrated device were found to be comparable with those obtained using a charge-coupled device (CCD) as a reference off-chip detector.

These results demonstrate that integrating the a-Si:H photosensors array with CL-LFIA technique provides compact, sensitive and low-cost systems for CL-based bioassays with a wide range of applications for in-field and point-of-care bioanalyses.

Keywords: Chemiluminescence, Lateral-flow immunoassay, Amorphous hydrogenated silicon photosensors, Integrated microdevice, Biosensors, Albuminuria.

Introduction

In the last years, Lateral Flow Immunoassays (LFIAs) have gained wide popularity and commercial success among the methods used for Point-of-Care (POC) applications. This analytical technique owes such achievements to the simplicity and rapidity of assay execution, as well as compactness, low cost and ease of use of LFIA devices. Indeed, LFIAs combine the advantages of immunoassays, such as applicability to a wide range of analytes, high specificity, high detectability and little or no need for preanalytical sample preparation, with the simplicity and rapidity of the immunochromatographic format [1].

Colloidal gold-based detection is most commonly employed in LFIA: the accumulation of labelled species in defined position along the strip determines the formation of coloured bands that are visually detected to provide a qualitative result (i.e., presence or absence of the analyte in the sample) or measured with a suitable device (an optical scanner or a smartphone-embedded camera) to provide objective, semi-quantitative information [2-4]. The use of alternative labels has recently gained wide acceptance, showing advantages in terms of assay sensitivity, but at the expense of assay simplicity and non-instrumental requirements. Many works reported the combination of LFIA technique with enzyme labels [5, 6], fluorescent nanoparticles [7-9], electrochemical probes [10] and magnetic nanoparticles [11], providing high assay sensitivity and reproducibility and wide linear ranges.

Chemiluminescence (CL) detection of enzyme-labelled biospecific reagents has been proposed as an ideal method for miniaturization and Point-of-care (POC) biosensor development thanks to its inherent sensitivity, specificity and rapidity [12, 13]. In particular, ultrasensitive CL detection combined with LFIA technique (CL-LFIA) has been demonstrated to provide superior analytical performance, yielding biosensors

characterized by high detectability, amenability to miniaturization, and short assay times. In addition, the instrumentation required for the readout of the CL signal from LFIA strips is much simpler and amenable to miniaturization with respect to that required for colloidal gold or fluorescence-based detection, since no external illumination is required. Inhomogeneous illumination of the LFIA strip is a greatly underestimated source of error in scanning- or imaging-based readers, which is instead avoided when CL detection is exploited. In addition, the intensity of illumination is also very important to achieve the best detectability, especially for fluorescence-based assays and this requires a large light power that hampers portability. [14]. To this end, light imaging systems based on a charge-coupled-device (CCD) camera [15-17] or even a smartphone's complementary metal-oxide semiconductor (CMOS) sensor [18] were employed for photons detection in CL-LFIAs.

Nevertheless, all of these approaches rely on "off-chip" coupling of the analytical support (the LFIA strip) and the detection device. While CCDs and CMOS are difficult to miniaturize into low-cost, portable detection devices, thin-film photodiodes have been successfully integrated in microfluidic systems in order to achieve ultrasensitive detection of analytes and to reduce the cost of diagnostic platforms. In particular, hydrogenated amorphous silicon (a-Si:H) photodiode arrays [19] and organic photodiodes (OPDs) [20] have been integrated into microfluidic devices and employed for measuring UV absorbance [21], fluorescence [22, 23], and CL signals [24-28].

Here we report for the first time a disposable CL-LFIA cartridge with integrated a-Si:H photosensors as CL detectors, which are controlled through a portable custom electronics. The add-on assembly comprises two parts: a glass slide on which an array of thin film a-Si:H photosensors has been deposited and a polydimethylsiloxane (PDMS) microfluidic cartridge that houses the LFIA strip and necessary reagents.

Once the operator has carried out the assay on the LFIA strip, the cartridge and the array of photosensors are assembled to perform the CL measurements in an integrated device.

In this work, we applied the developed biosensor for the quantitative detection of human serum albumin (HSA) in urine samples, which is considered a biomarker suitable to identify and monitor patients with kidney damage [29]. Normal HSA level in urine is lower than 25 mg L^{-1}. A higher level of HSA corresponds to the situation of microalbuminuria (in the concentration range between 25-200 mg L^{-1}) or macroalbuminuria (above 200 mg L^{-1}) [30].

Indeed, the level of urinary albumin excretion indicates kidney damage and it is recognized as a risk factor for progression of kidney disease and damage [29]. In particular the condition of microalbuminuria can be used to predict diabetic nephropathy [31]. Diabetes is a chronic illness that requires continuing medical care and patient self-management education to prevent acute complications and to reduce the risk of long-term complications. Generally, while Type I diabetes is manifested by acute symptoms such as markedly elevated blood glucose levels, Type II diabetes is frequently not diagnosed until complications appear. Diabetic nephropathy occurs in 20–40% of patients with diabetes and is the single leading cause of end-stage renal disease (ESRD). Persistent microalbuminuria has been shown to be the earliest stage of diabetic nephropathy in Type I diabetes and a marker for development of nephropathy in Type II diabetes. Patients with microalbuminuria who progress to macroalbuminuria are likely to progress to ESRD over a period of years [32]. The possibility to promptly detect kidney damage allows starting treatment when the damage is minimal and reversible and the monitoring of urinary albumin represents a principal component of treatment for both Type I and Type II diabetes mellitus. [33].

Moreover, higher rates of cardiovascular disease (CVD) are seen in patients with moderate and even mild renal dysfunction. Recent studies have indicated that even modest elevations in serum creatinine and urinary albumin excretion are associated with increased CVD risk, not only in subjects with diabetes or hypertension but also in the general population [34]. Therefore monitoring HSA can be useful for both diabetic and healthy patients in order to prevent future renal and cardiovascular adverse events [35].

The developed assay must therefore provide reproducible quantitative information in a very wide dynamic range in order to detect disease-related variations.

We optimized an indirect competitive immunoassay, in which HSA in urine and HSA immobilized on the nitrocellulose membrane compete for anti-HSA antibody. The detection is performed using horseradish peroxidase (HRP)-labelled secondary antibodies and adding the CL luminol/enhancer/hydrogen peroxide cocktail.

The proposed biosensor allows objective and accurate quantification of HSA in urine samples in the relevant physiological range, thus enabling rapid and reliable identification of those samples requiring confirmatory analysis.

Materials and methods

Chemicals

Polyclonal anti-human Albumin antibody produced in rabbit, polyclonal anti-peroxidase (HRP) antibody produced in rabbit, HRP-labeled goat anti-rabbit immunoglobulin, human serum albumin and bovine serum albumin were purchased from Sigma-Aldrich (St. Louis, MO).

All other reagents were of analytical grade and were used as purchased.

The SuperSignal ELISA Femto CL substrate for HRP was obtained from Thermo Fisher Scientific, Inc. (Rockford, IL).

Nitrocellulose membranes (Hi-flow180 A4 sheet) and cellulose adsorbent pads (20 x 300 mm) were bought from Merckmillipore (Billerica, MA). Sample pads were Standard 14 glass fiber pads (22 x 300 mmm) from Whatman and were purchased from GE Healthcare Life Sciences (Buckinghamshire, UK).

Phosphate buffered saline (PBS) was prepared as follows: 10 mmol L^{-1} Na_2HPO_4, 2 mmol L^{-1} KH_2PO_4, 137 mmol L^{-1} NaCl, 2.7 mmol L^{-1} KCl (pH 7.4).

Synthetic urine was prepared as previously described [36].

LFIA strips preparation

Assay strips for LFIA were prepared by using A4 sheets of nitrocellulose membranes with transparent backing. The membranes were previously cut into 2.5 cm high sections (250 x 297 mm) and the human serum albumin (T-line) and the rabbit anti-peroxidase antibody (C-line) were immobilized, from bottom to top of the strip, keeping a distance of 5.5 mm. After line dispensing, two adhesives were pasted onto the top and the bottom of the membrane to assemble the sample and adsorbent pads, respectively. Overlapping of the adhesive and pads with the membrane was maintained as narrow as possible that resulted in a transparent window of 140 mm high. Finally the membranes were cut into strips of 5.4 mm width.

Photosensor array and electronic read-out board

As previously described [28], the photosensors array is a 5x6 matrix of a-Si:H diodes. Each photosensors is a p-type/intrinsic/n-type structure grown on glass substrate by a three chamber high-vacuum Plasma Enhanced Chemical Vapor Deposition (PECVD).

In particular, the fabrication process has been implemented with the following technological steps: a. cleaning of a 5 x 5 cm^2 glass substrate by piranha solution, b) deposition by magnetron sputtering and patterning by photolithographic processes of a 200 nm-thick layer of Indium Tin Oxide (ITO) acting as front electrode of the a-Si:H photosensor; c) deposition of the a-Si: layers; d) deposition by vacuum evaporation of a 30/150/30 nm-thick stack of Al/Cr/Al as back contact; e) patterning of the metal stack and of the a-Si:H layers to define the photosensor geometries; d) deposition and patterning of a 5 μm-thick layer of SU-8 3005 acting as insulation layer; e) deposition by vacuum evaporation and patterning by photolithographic processes of a 30/150/30 nm-thick stack of Al/Cr/Al to define the electrical connections to the metal pad of the back contact. In this device configuration, light is impinging on the a-Si:H photosensor through the glass and the ITO layer.

A qualitative illustration of the cross section of one photosensor is reported in Figure 1, also showing a picture of the photosensors array.

The light- grey squares in the middle of the picture are the 30 a-Si:H photosensors. The C-shaped line is the metal back contact, which is common to all the photosensors, while the ITO transparent front contacts (one for each diode) end with the short metal contacts visible on the lower edge of the glass substrate.

These metal contacts allow an easier alignment of the photosensor array with the card edge connector (SAMTEC MB1–150–01–L–S–02–SL), which in turn is connected through a simple interface board to the read-out electronic. The input stage of read-out circuit is based on a 8-channel, 20-bit analog-to-digital converter (DDC118 from Texas Instruments), which receives the currents generated by the photodiodes, provides the current-to-voltage conversion through a charge sensing amplifier and digitizes them thanks to the internal sigma-delta modulator. The results are presented at the output

of a synchronous serial interface driven by a clock signal. The master of the read-out circuit is a PIC18F4550 microcontroller (from Microchip) that has two main functions: 1) providing the timing and control signals to the DDC; 2) ensuring the communication to a PC. A software running on the computer sets all the measurement parameters through a USB port, stores and visualizes the measurement data.

Analytical device

The disposable analytical cartridge comprises a PDMS fluidic element that houses the LFIA nitrocellulose membrane and contains all the reagents necessary for the analysis (Figure 2).

In more detail, the fluidic element contains three reagent reservoirs: a 50-μL reservoir for the immunoreagents solution and two 40-μL reservoirs for the two components of the SuperSignal ELISA Femto HRP CL cocktail. The immunoreagents solution was PBS containing 3% (w/v) BSA, anti-HSA antibody (diluted 1: 2000, v/v) and HRP-labelled anti-rabbit antibody (diluted 1:5000, v/v).

In addition, hollow spaces were engraved in the PDMS fluidic element in the correspondence of the LFIA strip to facilitate water evaporation, thus further promoting the capillary flow along the strip. A 3D-printed ABS frame encloses the PDMS element in order to assure its reproducible positioning in the correspondence of the photodiodes array. This is critical to assure the correct readout of the CL signals. Indeed, four aligned photodiodes was used to measure the CL signal from the strip: two of them, placed in the correspondence of the test and control lines of the strip, respectively, measured the analytical signals; the others were placed in blank areas of the LFIA strip (i.e., just before and after the lines) to perform background correction (Figure 3).

Since this approach has not previously been used to acquire CL signals from LFIA membranes, the analytical performance of the photodiodes was compared with that of a conventional ultrasensitive charge coupled device (CCD) camera (MZ-2PRO from MagZero, Pordenone, Italy, equipped with a Sony ICX285 sensor), coupled with a round fiber optic taper (25/11 mm size, Edmund Optics, Barrington, NJ) placed in contact with the CCD sensor. This set-up had been previously used to develop CL-LFIA methods in a contact imaging configuration [15, 17].

Assay procedure

For the analysis, 10 μL of sample was transferred with a syringe into the prefilled immunoreagents reservoir, in order to mix the sample with the solution of rabbit anti-HSA antibody and HRP-labelled anti-rabbit antibody. By squeezing the reservoir, the solution reached the sample pad and began flowing across the membrane where the immunoreactions took place. Upon complete migration of the solution (30 min), the CL substrate was added to the strip by simultaneously pushing the two dedicated reservoirs. After inserting the cartridge on the photodiodes array (Figure 3) and enclosing the system in a dark box, the CL signals were monitored through consecutive 200-ms acquisitions (total acquisition time 2 minutes).

Calibration curves for HSA were produced employing standard solutions prepared by adding HSA to synthetic urine to the desired concentration, comprised between 0 (blank) and 2500 mg L^{-1}.

To obtain quantitative information, the mean photon emission intensity was measured in the areas corresponding to C-line and T-line of the LFIA strip. In addition, background signal was recorded in two areas of the nitrocellulose membrane: just before and after the lines (Figure 3).

The mean background was subtracted from the CL signals recorded for the C-line and T-line , then the T-line/C-line ratio was calculated for each concentration. and converted into B/B_0 ratio by dividing it for the T-line/C-line ratio measured in the absence of the target analyte (B_0, i.e. maximum T-line/C-line value). Then, the T-line/C-line ratio obtained for each analyte concentration (B) was divided for the T-line/C-line ratio obtained in the absence of the target analyte, which corresponds to the maximum T-line/C-line value (B_0). Finally, B/B_0 ratio, which represents the fraction of the tracer that has been displaced by a specific concentration of the analyte, was plotted against the log of analyte concentration obtaining a sigmoidal curve that is described by a four-parameter logistic function.

In particular, a non-linear regression analysis was performed using the following equation:

$$Y = Y_0 + \frac{(Y_1 - Y_0)}{(1 + 10^{[(b-x)c]})}$$

where $Y = B/B_0$, Y_0 = bottom asymptote (the ∞ dose), Y_1 = top asymptote (the 0 dose), x = log of analyte concentration (mg L^{-1}), b = log of analyte at midpoint of curve (mg L^{-1}), c = slope.

The intensity of the CL signal of the C-line above a defined threshold value was exploited to confirm the validity of the assay. The threshold value was defined by measuring the blank signal in 15 different strips and calculating the average blank signal plus 10 times its standard deviation.

To obtain the analyte concentration in real samples, B/B_0 value was calculated as described above and interpolated on a stored calibration curve.

Samples and spiked samples preparation

Human urine samples were kindly provided by the Laboratory of Clinical Chemistry and Microbiology of the Umberto I Hospital (Turin, Italy). Clinical samples were available for research purposes according to Italian privacy law.

Confirmatory analyses were performed using the reference method Multigent Microalbumin assay on an Architect Ci8200® analyzer (Abbott, Abbot Park, IL, USA).

3. Results and discussion

Lateral flow immunoassays represent a well-established and very appropriate technology for developing easy-to-use and robust POC analytical devices. Their coupling with CL detection has previously shown to improve analytical performance, including a higher sensitivity and the ability to provide quantitative information [15-18]. This would therefore bring the range of applications as well as the analytical performance of LFIAs closer to that of conventional analytical instrumentation. Nevertheless, CL-LFIAs require multiple steps and different reagents, thus LFIAs devices should be properly designed to maintain the peculiarities of the LFIA technique, such as its amenability for on-field application. In this context, it is also important to implement simple, easy-to-use and cheap but still highly sensitive signal detectors to fully exploit the quantitative potentiality of CL detection [18]. Indeed, integration of LFIAs with objective measurement technologies is considered one of the key aspects for next generation LFIAs [1].

In this work we propose for the first time an array of thin-film a-Si:H photosensors as detector for CL-LFIA. The analytical performances of these sensors has been previously demonstrated in bioanalytical applications such as enzyme assays, immunoassays and gene probe assays [19, 26, 27]. In order to develop a fully integrate device, we coupled the miniaturized detector with a disposable PDMS microfluidic cartridge that houses the LFIA strip and all the reagents required for performing the analysis and enables easy manual dispensing of the reagents according to the analytical protocol. This analytical device will thus combine the simplicity and specificity of LFIA assays with the sensitivity of CL as reporting technique and with the low cost and easy integration of thin-film a-Si:H photosensors in miniaturized, portable instrumentation.

Photosensor array and electronic read-out board

The photosensor array was designed to enable high detectability for the CL signals. In particular, basing on simulation results performed with a numerical simulator previously developed by the authors [37], the p-layer thickness has been set to 10 nm. Indeed, taking into account that the active region is the intrinsic layer, while the doped layers do not contribute to the photocurrent signal, thickness and energy gap of the p-doped layer have to be carefully designed. In particular, this region has to be thick enough to sustain the built-in potential, but, at the same time, as thin as possible to reduce the absorption of the radiation.

In addition, in order to further reduce its absorption, the p-doped film has been grown by a mixture of silane, diborane and methane. Indeed, the methane presence ensures an increase of the energy gap (from 1.72 to about 2 eV) and therefore a decrease of the carriers photogenerated in this layer.

The area of each diode (2 x 2mm^2) and the pitch of the array (5 mm), which result in a minimum distance between the photosensors equal to 3 mm, were adopted to ensure a reduced cross talk effect [38].

The photosensor characterization has been carried out measuring the current-voltage characteristics (IV) in dark condition and the spectral response in the visible range. The IV curves have been measured by a Source Measure Unit Keithley 236 in a metal shielded box to avoid the effect of electromagnetic interferences. The spectral response has been measured by a double-arm optical set-up, which includes a Jobin-Yvon SPEX monochromator, a halogen lamp as radiation source, a beam splitter, a calibrated crystalline photodiode from Hamamatsu and lenses for focusing the light. Two Keithley 236 Source Measure Units read-out the photocurrents of the reference

diode and of the a-Si: photosensors. We found a very well reproducibility over the all photosensors of the array with standard deviations around 3% for both the IV and responsivity curves.

From the IV characteristics, we found that the dark current at small reverse voltage (few mV) is around 2 pA. This value corresponds to a current noise equal to 1 fA.

Results of the spectral response are reported in Figure 4, where we infer that at 425 nm, the wavelength corresponding to the emission peak of the HRP, the responsivity R is equal to 170 mA/W.

From the characterization of the whole system (read-out electronics connected to the photosensors), we found that in the operating conditions utilized during the CL measurements (200 ms integration time and 50 pF integration capacitance), the total current noise in is around 40 fA. Taking into account the definition of noise equivalent power (NEP), i.e. the incident power that provides an output signal equal to the system noise in dark condition, we found that the minimum detectable power is 0.235 pW .

$$NEP = \frac{\sqrt{\overline{i_n^2}}}{R}$$

Assuming that this power is due to photons at 425 nm we deduce that the minimum detectable number of incident photons per second is 5×10^5 for each photosensor.

CL-LFIA assay principle

In order to achieve high detectability and quantitative information, an indirect competitive CL-LFIA assay was developed for HSA detection in urine (Figure 3). The analyte in the sample (or in the standard solution) migrates along the LFIA nitrocellulose membrane together with rabbit anti-HSA antibody and HRP-labelled anti-

rabbit antibody. In correspondence of the T-line, the analyte competes with HSA immobilized on the nitrocellulose membrane for binding to the fixed and limited amount of anti-HSA in solution. At the same time, the HRP-labelled anti-rabbit antibody binds to the anti-HSA antibody captured in the T-line area. Afterwards, unbound reagents continue to migrate until they reach the C-line, where the excess of HRP-labelled anti-rabbit antibody is captured by immobilized anti-HRP antibody. In the detection step, a CL cocktail for HRP was added to the strip and the resulting CL signal from both lines was recorded using the photodiodes array.

Being a competitive type assay format, the intensity of the CL signal measured in the T-line is inversely related to the amount of HSA. The observation of a CL signal above a threshold value (blank signal plus 10 times its standard deviation) in the correspondence of the C-line confirms the correct assay execution.

To obtain quantitative information, the T-line/C-line ratio was calculated for each HSA concentration, upon subtracting each signal of the mean background signal. The T-line/C-line ratio allows to normalize the CL signal of the T-line with respect to that of the C-line of the same strip, taking into account environmental and matrix factors that might affect the intensity of the CL signal (i.e. changes in ambient temperature, the presence of HRP inhibitors in the sample, etc) thus improving the reproducibility of the assay.

It is worth noting that, despite the fact that the target analyte is a protein, a competitive immunoassay was employed instead of a non-competitive, sandwich-type immunoassay. Such format was preferred to reduce the overall cost of the assay, as a sandwich immunoassay would require two different specific anti-HSA antibodies, while in our assay only one specific antibody was required. In addition, the amount of capture antibody immobilized in the T-line of a LFIA strip for a typical sandwich immunoassay

is 10–30 mg cm^{-2}, which is 25–100 times that used in microtiter plate sandwich immunoassays [39]. In our assay, HSA was immobilized in the T-line area and the antibodies required for the assay were added in solution. This approach reduced the consumption of expensive immunospecific reagents, which is considered the main factor influencing the overall test cost-effectiveness.

Cartridge design

As previously stated, the addition of multiple reagents is required to perform CL-LFIAs. Therefore, the PDMS microfluidic cartridge (Figure 2) comprises reservoirs connected to the LFIA sample pad through fluidic channels that allow manual dispensing of the reagents onto the LFIA strip according to the analytical protocol. In more detail, three reagent reservoirs, which contain the immunoreagents (anti-HSA and HRP-labelled anti-rabbit antibodies) and the two components of the CL HRP detection cocktail, respectively, were engraved in the PDMS module. The PDMS cartridge, together with the ABS 3D printed frame allows reproducible positioning of the LFIA strip on the a-Si:H photosensors array.

Since the components of the CL HRP cocktail are in excess, while a reproducible amount of sample and immunoreagents must be delivered to the strip, the reservoir containing the immunoreagents was placed in close proximity to the strip to reduce the dead volume of the fluidic channel. Indeed, it is known that reproducibility in LFIAs largely depends on the accurate delivery of sample to the strip and the subsequent movement of the sample and conjugates through the device to the reaction matrix [40]. The components of the CL cocktail (which accomplishes two different tasks, i.e., washing unbound immunoreagents from the strip and triggering the HRP-catalysed CL reaction) are delivered to the strip by simultaneously pushing their reservoirs and mix

upon dispensing onto the sample pad before flowing along the LFIA strip. To increase washing efficiency, the CL cocktail components are delivered to the strip at half-length of the sample pad.

LFIA optimization

Concentration of the immunoreagents were optimized to achieve limit of detection (LOD) and dynamic range suitable for detecting HSA in the relevant physiological range. In addition, similar CL intensities must be obtained in the T-line and C-line to prevent excessive interference between the signals.

The optimal concentration of HSA (1 mg/mL) and anti-HRP antibody (1:1000 v/v dilution) to be immobilized onto the nitrocellulose strip, as well of rabbit anti-HSA (1:2000 v/v dilution) and HRP-labelled anti-rabbit antibody (1:5000 v/v dilution), were selected (Supplementary material). These concentrations ensure the absence of cross-talk phenomena between C-line and T-line and produce a calibration curve that allows direct analysis of urine samples and discrimination between diagnostically relevant urinary HSA levels.

Signal detection

The production of a LFIA strip requires lamination of multiple materials into one unit. Lamination is usually performed by assembly of the LFIA components on a backing material that provides rigidity and easy handling of the strip. The backing materials are typically opaque white polystyrene or other plastic materials coated with an adhesive. On the contrary, a LFIA strip with transparent backing support was produced in this work to ensure high photon transmission, thus enabling direct measurement of the CL

signal from the LFIA strip employing the array of a-Si:H photosensors aligned below the strip (Figure 3).

It is also worth noting that the nitrocellulose strip is also opaque, but it can be assumed that the immobilization of immunoreagents, and thus the consequent immunoreactions, take place along the whole thickness of the strip. Therefore, CL signals can be measured indifferently form both sides without significant loss.

To further improve light collection efficiency and obtain a compact and miniaturized device, the LFIA strip enclosed in the transparent PDMS cartridge was placed in close contact with the photosensors array. In the proposed system the distance between the place where the CL reaction takes place and the detection site is extremely short (in the order of 1mm, sum of the glass thickness and the bottom PDMS layer). This avoids the use lens for focusing the emitted radiation and allows a reduction of the system complexity and a high degree of miniaturization.

The configuration used for the measurement of CL signal thus leads to a hand-held device providing objective and accurate quantitative information. The device has no moving parts, differently from scanning systems, which increase its robustness.

The array of photosensors controlled by the custom read-out electronics allowed to simultaneously measure the CL signal in all the relevant areas of the nitrocellulose membrane (Figure 3), making it possible to obtain the values of CL signals related to T-line, C-line and their adjacent areas (for measuring the background signal). For this purpose, all the photosensors must respond equally to light and the absence of crosstalk phenomena among adjacent photosensors must be assessed. The performances of the photosensors array in terms of background noise, detectability of chemiluminescent system and crosstalk phaenomena, had been previously evaluated [27]. Since this is the first report about coupling thin-film photosensors with CL-LFIA,

light measurements were also performed by imaging with a portable, thermoelectrically-cooled CCD camera that had already proved to be suitable detector for CL-LFIA approach in previously works [15, 17]. The results showed that the array of photosensors allowed to measure CL intensity of each interest area without significant crosstalk and that its performance was similar to that obtained using the CCD camera. In Figure 3S (Supplementary Material) CL signals obtained in correspondence of the T-line and C-line of various LFIA strips using a-Si:H photosensors are plotted against the same signals acquired with CCD camera in a "contact" imaging configuration. . There is a clear correspondence between the signals measured by the two different platforms, showing that, as the CCD camera, even photosensors are suitable for the coupling with the CL-LFIA technique. This result is very encouraging considering that the a-Si:H photosensors were employed at room temperature (about 25°C) while the CCD sensor was cooled down to 5°C to decrease the background signal, which is mainly due to thermal noise.

Another advantageous aspect is that the digital memory occupancy of the data measured using a-Si:H photosensors is significantly lower than those of data generated by image-based systems. This represents a benefit not only for the data storage, but also for the algorithm complexity and computing time for data analysis.

Furthermore, the cost of production of the detector is much lower when manufactured at a large scale, as compared with CCD-based detectors. Indeed, the a-Si:H technology is mature, inexpensive and suitable for different kinds of substrate owing to its low deposition temperature. In particular, the thermal budget for the deposition of amorphous silicon (which occurs at temperature below 300°C) is much lower than the thermal budget required by crystalline silicon, whose process temperature can reach 1000°C.

It is worth noting that in this work 4 out of 30 a-Si:H photosensors of the array were employed. In the future, dedicated arrays will be produced for CL-LFIA applications.

Calibration curve

Calibration curves were generated using HSA standard solutions in the range 0 - 2500 ng/mL, both in synthetic urine and in PBS to evaluate the matrix effect.

The calibration curves are reported in Figure 5. Being a competitive type format, a typical sigmoidal calibration curve was obtained by reporting the signal versus the logarithm of HSA concentration. Instead of the T-line signal alone, the T-line/C-line ratio was calculated and plotted against the analyte concentration to improve assay reproducibility by taking into account environmental and matrix factors that might affect the intensity of the CL signal (e.g. changes in ambient temperature, presence of HRP inhibitors in the sample). In addition, to confirm the validity of the assay a C-line minimum signal threshold above background was defined.

The results of three repeated calibration curves demonstrated a good reproducibility with a coefficient of variation associated with each point of the calibration curve below 20% both in buffer and in urine matrix. The limit of detection (LOD) was estimated as the concentration corresponding to the blank T-line/C-line value minus three times its standard deviation. The obtained values were 2.5 mg L^{-1} in synthetic urine and 3.1 mg L^{-1} in PBS while the dynamic ranges of the method were 2.5-850 mg L^{-1} for synthetic urine and 3.1-842 mg L^{-1} in PBS, therefore showing a negligible matrix effect (Figure 5). Moreover, no significant differences were observed by comparing calibration curves obtained using the a-Si:H photodiode array and the CCD sensor as CL detectors (Figure 5).

Figure 5 also shows dashed lines in correspondence of the HSA urinary levels that enable discrimination between normal subjects and those affected by micro- or macroalbuminuria. The assay was optimized in order to obtain a dynamic range of the calibration curve assay suitable for direct analysis of urine samples and quantitative analyte measurements in all the levels relevant for diagnostic purposes. It is worth noting that lower limits of detection of the assay could be obtained employing different experimental conditions, but these were not selected in this work to avoid the need for diluting the urine sample prior to the analysis, thus increasing the POC applicability of the test.

Samples

To confirm the accuracy of the proposed method, urine samples provided by the Umberto I Hospital (Turin, Italy) were analysed using HSA calibration curves generated in synthetic urine. The results (mean of three independent measurements) were compared with those obtained using a reference turbidimetric immunoassay, routinely employed in the Laboratory of Clinical Chemistry and Microbiology of the Umberto I Hospital (Turin, Italy). A good agreement between CL-LFIA and reference method results was found for all samples (Figure 6). In detail, recovery values ranging from 85% to 112% and coefficients of variation below 20% were obtained, proving the reliability and applicability of the proposed CL-LFIA for quantitative determination of HSA in urine samples.

These results provide a demonstration of the suitability of the proposed biosensor for the direct analysis of urine samples in POC settings. Its compactness and integration make it a user-friendly analytical device suitable for the quantitative evaluation of the level of urinary albumin excretion, thus for early diagnosis of diabetic nephropathy and

prognosis of progression to ESRD. This will facilitate screening procedures, thus enabling early stage treatment and preventing irreversible kidney damage.

Conclusions

A novel integrated device was developed by coupling a PDMS cartridge, containing the LFIA strip and all the reagents necessary to complete the analysis, with an array of thin film a-Si:H photosensors. The device was exploited to perform quantitative analysis of HSA in urine samples employing a CL-LFIA assay, showing its suitability for POC diagnostic applications.

The developed biosensor overcomes the main shortcomings of conventional LFIAs, such as inconvenience in manual documentation and subjective interpretation, only allowing qualitative measurements and often leading to false negative and false positive results.

Thanks to the solutions adopted in the device development, the features requested for POC applicability were fulfilled. In particular, reagent embedding and Si:H photosensors integration provided speed of analysis, simplicity of operation and device portability. In addition, use of CL detection and optimization of assay experimental parameters enabled direct sample quantitative analysis, avoiding time-consuming sample preparation steps.

Taking advantage of the convergence between CL-LFIA and thin film photosensor deposition technologies, the reported device implements features and benefits that cost-effectively match the needs for POC diagnostics applications.

Compliance with Ethical Standards

Conflict of Interest: The authors declare that they have no conflict of interest.

Acknowledgements

We are very grateful to Scriba Nanotecnologie S.r.l. (www.scriba-nanotec.com) for strict collaboration and fruitful scientific discussion related to the design and production of the polydimethylsiloxane cartridge.

Financial support was provided by the Italian Ministry of Instruction, University and Research: PRIN 2010 project prot. 20108ZSRTR “ARTEMIDE (Autonomous Real Time Embedded Multi-analyte Integrated Detection Environment): a fully integrated lab-on-chip for early diagnosis of viral infections”.

References

1. Wong RC, Tse HY. Lateral Flow Immunoassay. New York: Humana Press; 2009.
2. Anfossi L, Calderara M, Baggiani C, Giovannoli C, Arletti E, Giraudi G. Development and application of a quantitative lateral flow immunoassay for fumonisins in maize. Anal Chim Acta 2010;682:104–9.
3. Smith JP, Sammons DL, Robertson SA, Snawder JE. Enhanced performance of methamphetamine lateral flow cassettes using an electronic lateral flow reader. J Occup Environ Hyg. 2015;12:45-50.
4. Lee S, Kim G, Moon J. Development of a smartphone-based reading system for lateral flow immunoassay. J Nanosci Nanotechnol. 2014;14:8453-7.

5. Adhikari M, Strych U, Kim J, Goux H, Dhamane S, Poongavanam MV, Hagstrom AEV, Kourentzi K, Conrad JC, Willson RC. Aptamer-phage reporters for ultrasensitive lateral flow assays. Anal Chem. 2015;87:11660-5.
6. Cho I-H, Bhunia A, Irudayaraj J. Rapid pathogen detection by lateral-flow immunochromatographic assay with gold nanoparticle-assisted enzyme signal amplification. Int J Food Microbiol. 2015;206:60-6.
7. Liang RL, Xu XP, Liu TC, Zhou JW, Wang XG, Ren ZQ, Hao F, Wu YS. Rapid and sensitive lateral flow immunoassay method for determining alpha fetoprotein in serum using europium (III) chelate microparticles-based lateral flow test strips. Anal Chim Acta 2015;891:277-83.
8. Chen YQ, Chen Q, Han MM, Liu JY, Zhao P, He LD, Zhang Y, Niu YM, Yang WJ, Zhang LY. Near-infrared fluorescence-based multiplex lateral flow immunoassay for the simultaneous detection of four antibiotic residue families in milk. Biosens Bioelectron. 2016;79:430-4.
9. Di Nardo F, Anfossi L, Giovannoli C, Passini C, Goftman VV, Goryacheva IY, Baggiani C. A fluorescent immunochromatographic strip test using quantum dots for fumonisins detection. Talanta 2016;150:463-8.
10. Sinawang PD, Rai V, Ionescu RE, Marks RS. Electrochemical lateral flow immunosensor for detection and quantification of dengue NS1 protein. Biosens Bioelectron. 2016;77:400-8.
11. Shi L, Wu F, Wen Y, Zhao F, Xiang J, Ma L. A novel method to detect Listeria monocytogenes via superparamagnetic lateral flow immunoassay. Anal Bioanal Chem 2015;407:529–35.
12. Seidel M, Niessner R. Chemiluminescence microarrays in analytical chemistry: a critical review. Anal Bioanal Chem. 2014;406:5589-612.

13. Mirasoli M, Guardigli M, Michelini E, Roda A. Recent advancements in chemical luminescence-based lab-on-chip and microfluidic platforms for bioanalysis. J Pharm Biomed Anal. 2014;87:36-52.
14. Faulstich K, Gruler R, Eberhard M, Lentzsch D, Haberstroh K. Handheld and portable reader devices for lateral flow immunoassays. In: Wong RC, Tse HY, editors. Lateral Flow Immunoassay. New York: Humana Press; 2009. pp. 157-83.
15. Mirasoli M, Buragina A, Dolci LS, Simoni P, Anfossi L, Giraudi G, Roda A. Chemiluminescence based biosensor for fumonisins quantitative detection in maize samples. Biosens Bioelectron. 2012;32:283–7.
16. Mirasoli M, Buragina A, Dolci LS, Guardigli M, Simoni P, Montoya A, Maiolini E, Girotti S, Roda A. Development of a chemiluminescence-based quantitative lateral flow immunoassay for on-field detection of 2,4,6-trinitrotoluene. Anal Chim Acta 2012;721:167–72.
17. Zangheri M, Di Nardo F, Anfossi L, Giovannoli C, Baggiani C, Roda A, Mirasoli M. A multiplex chemiluminescent biosensor for type B-fumonisins and aflatoxin B1 quantitative detection in maize flour. Analyst 2015;140:358-65.
18. Zangheri M, Cevenini L, Anfossi L, Baggiani C, Simoni P, Di Nardo F, Roda A. A simple and compact smartphone accessory for quantitative chemiluminescence-based lateral flow immunoassay for salivary cortisol detection. Biosens Bioelectron. 2015;64:63–8.
19. Caputo D, de Cesare G, Dolci LS, Mirasoli M, Nascetti A, Roda A, Scipinotti R. Microfluidic chip with integrated a-Si:H photodiodes for chemiluminescence-based bioassays. IEEE Sens J. 2013;13:2595–602.

20. Pires NMM, Dong T. Measurement of salivary cortisol by a chemiluminescent organic-based immunosensor. Biomed Mater Eng. 2014;24:15–20.
21. de Cesare G, Caputo D, Nascetti A, Guiducci C, Riccò B. a-Si: H ultraviolet sensor for deoxyribonucleic acid analysis. Appl Phys Lett. 2006;88:083904–6.
22. Caputo D, de Cesare G, Nascetti A, Negri R. Spectral tuned amorphous silicon p-i-n for DNA detection. J Non-Cryst Solids 2006;352:2004–6.
23. Caputo D, de Cesare G, Fanelli C, Nascetti A, Ricelli A, Scipinotti R. Amorphous silicon photosensors for detection of Ochratoxin A in wine. IEEE Sens J. 2012;12:2674–9.
24. Novo P, Prazeres DMF, Chu V, Conde JP. Microspot-based ELISA in microfluidics: chemiluminescence and colorimetry detection using integrated thin-film hydrogenated amorphous silicon photodiodes. Lab Chip 2011;11:4063–71.
25. Novo P, Moulas G, Prazeres DMF, Chu V, Conde JP. Detection of ochratoxin A in wine and beer by chemiluminescence-based ELISA in microfluidics with integrated photodiodes. Sensor Actuat B-Chem. 2013;176:232–40.
26. Caputo D, de Cesare G, Scipinotti R, Mirasoli M, Roda A, Zangheri M, Nascetti A. Chemiluminescence-based micro-total-analysis system with amorphous silicon photodiodes. Lect Notes Electr Eng. 2014;268:207–11.
27. Mirasoli M, Nascetti A, Caputo D, Zangheri M, Scipinotti R, Cevenini L, de Cesare G, Roda A. Multiwell cartridge with integrated array of amorphous silicon photosensors for chemiluminescence detection: development, characterization and comparison with cooled-CCD luminograph. Anal Bioanal Chem. 2014;406:5645-56.

28. Zangheri M, Mirasoli M, Nascetti A, Caputo D, Bonvicini F, Gallinella G, de Cesare G, Roda A. Microfluidic cartridge with integrated array of amorphous silicon photosensors for chemiluminescence detection of viral DNA. Sens Biosens Res. 2016;7:127-32.
29. Miller GW, Bruns DE, Hortin GL, Sandberg S, Aakre KM, McQueen MJ, Itoh Y, Lieske JC, Seccombe DW, Jones G, Bunk DM, Curhan GC, Narva AS. Current issues in measurement and reporting of urinary albumin excretion. Clin Chem. 2009;55:24–38.
30. Seegmiller JC, Barnidge DR, Burns BE, Larson TS, Lieske JC, Kumar R. Quantification of urinary albumin by using protein cleavage and LC-MS/MS. Clin Chem. 2009;55:1100–7.
31. Mogensen CE, Christensen CK, Vittinghus E. The stages in diabetic renal disease. With emphasis on the stage of incipient diabetic nephropathy. Diabetes 1983;32:64-78.
32. American Diabetes Association. Standards of medical care for patients with diabetes mellitus. Diabetes Care 2003;26:S33-S50.
33. Burtis CA, Ashwood Tietz ER. Textbook of clinical chemistry. 3rd ed. W.B. Saunders Company; 1999.
34. Adachi H. Microalbuminuria is an independent prognostic information for cardiovascular disease. Atherosclerosis 2014;237:106–7.
35. Basi S, Fesler P, Mimran A, Lewis JB. Microalbuminuria in type 2 diabetes and hypertension. Diabetes Care 2008;31:S194-S201.
36. Miró-Casas E, Farré Albaladejo M, Covas M-I, Rodriguez JO, Menoyo Colomer E, Lamuela Raventós RM, de la Torre R. Capillary gas chromatography–mass

spectrometry quantitative determination of hydroxytyrosol and tyrosol in human urine after olive oil intake. Anal Biochem. 2001;294:63-72.

37. Caputo D, Forghieri U, Palma F. Low-temperature admittance measurement in thin film amorphous silicon structures. J Appl Phys. 1997;82:733-41.
38. Caputo D, de Angelis A, Lovecchio N, Nascetti A, Scipinotti R, de Cesare G. Amorphous silicon photosensors integrated in microfluidic structures as a technological demonstrator of a Lab-on-Chip system. Sens Biosens Res. 2015;3:98-104.
39. Brown MC. Evolution in lateral flow–based immunoassay systems. In: Wong RC, Tse HY, editors. Lateral Flow Immunoassay. New York: Humana Press; 2009. pp. 1-33.
40. O'Farrell B. Antibodies: Key to a robust lateral flow immunoassay. In: Wong RC, Tse HY, editors. Lateral Flow Immunoassay. New York: Humana Press; 2009. pp. 59-74.

Figure captions

Figure 1. Cross section of the photosensor structure, showing the thickness of the different layers. The metal back contact is a double stack of Cr/Al/Cr layers with thicknesses equal to 30/150/30 nm, respectively. Inset: picture of the photosensor array fabricated on a 5 x 5cm^2 glass substrate.

Figure 2. a) Picture of the PDMS microfluidic cartridge enclosing the CL-LFIA strip and reagents and equipped with the ABS 3D printed frame. b) Exploded view of the components of the PDMS microfluidic cartridge components.

Figure 3. a) Scheme of the CL-LFIA strip showing the assay principle (top) and the position of the photosensors below the strip (bottom). b) Picture of the complete device,

comprising the PDMS microfluidic cartridge with integrated a-Si:H photosensors and the custom readout electronics. c) Typical output signal obtained for a single CL-LFIA strip.

Figure 4. Typical spectral response of the a-Si:H photosensors. A very good reproducibility (relative standard deviation around 3%) has been achieved.

Figure 5. a) CL-LFIA calibration curves for HSA obtained by measuring the CL signals with the integrated a-si:H photosensors (black) or with a cooled CCD-based device employed in a “contact” imaging configuration (red). b) CL-LFIA calibration curves for HSA obtained by preparing the HSA standard solutions in PBS (blue) or in synthetic urine (orange). c) Typical signal outputs for a series of CL-LFIA strips employed to construct a calibration curve for HSA. T-line signals are shown in black, with the corresponding HSA concentration, while C-line signals are shown in grey.

Figure 6. Results obtained by analysing urine samples with the integrated device for CL-LFIA, as compared with those obtained with a reference immunoturbidimetric assay. Samples with HSA in the normal range are shown in green, while samples with HSA indicating microalbuminuria and macroalbuminuria are shown in orange and red, respectively.

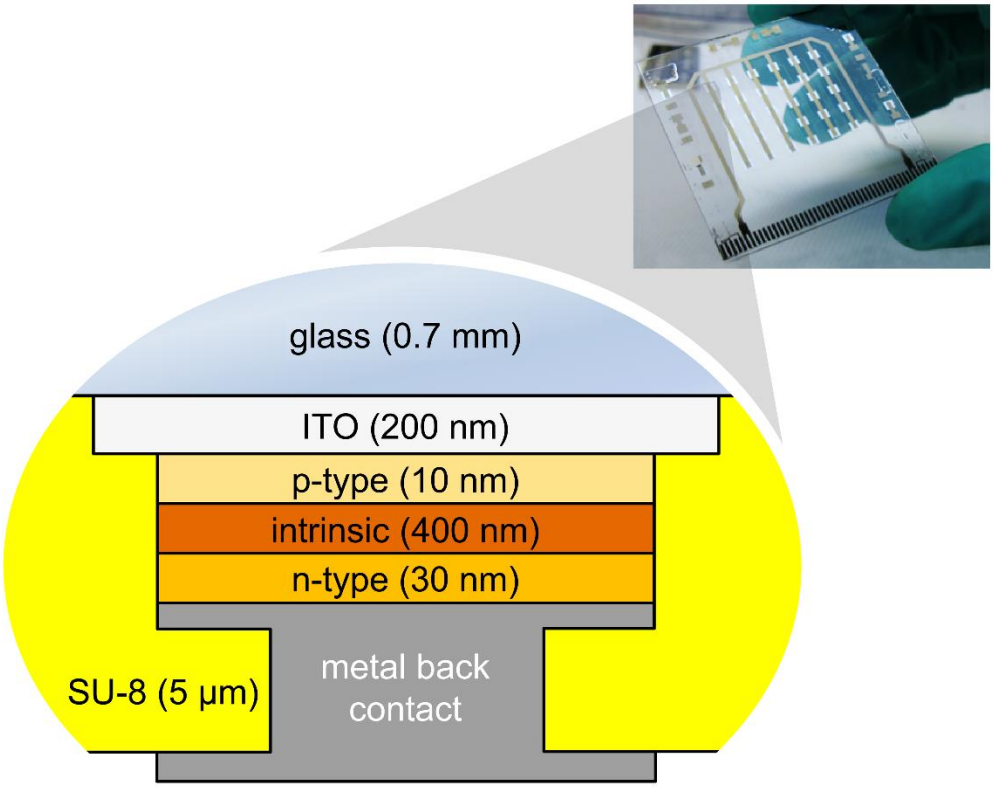
glass (0.7 mm)
ITO (200 nm)
p-type (10 nm)
intrinsic (400 nm)
n-type (30 nm)
SU-8 (5 µm)
metal back
contact

Figure 1

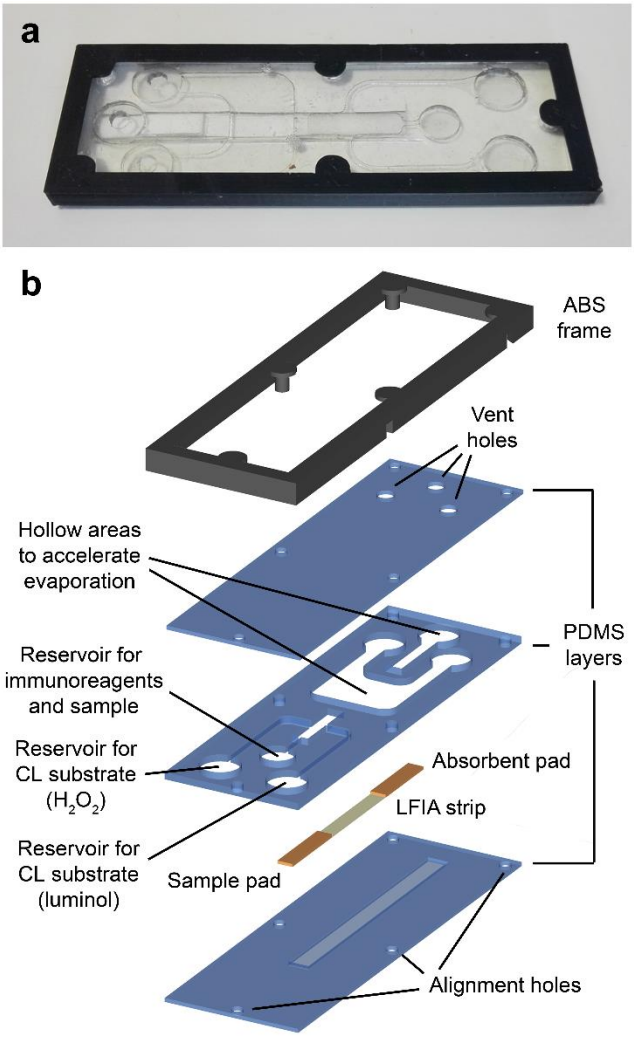
a
b
ABS
frame
Vent
holes
Hollow areas
to accelerate
evaporation
PDMS
layers
Reservoir for
immunoreagents
and sample
Reservoir for
CL substrate
(H_2O_2)
Absorbent pad
LFIA strip
Reservoir for
CL substrate
(luminol)
Sample pad
Alignment holes

Figure 2

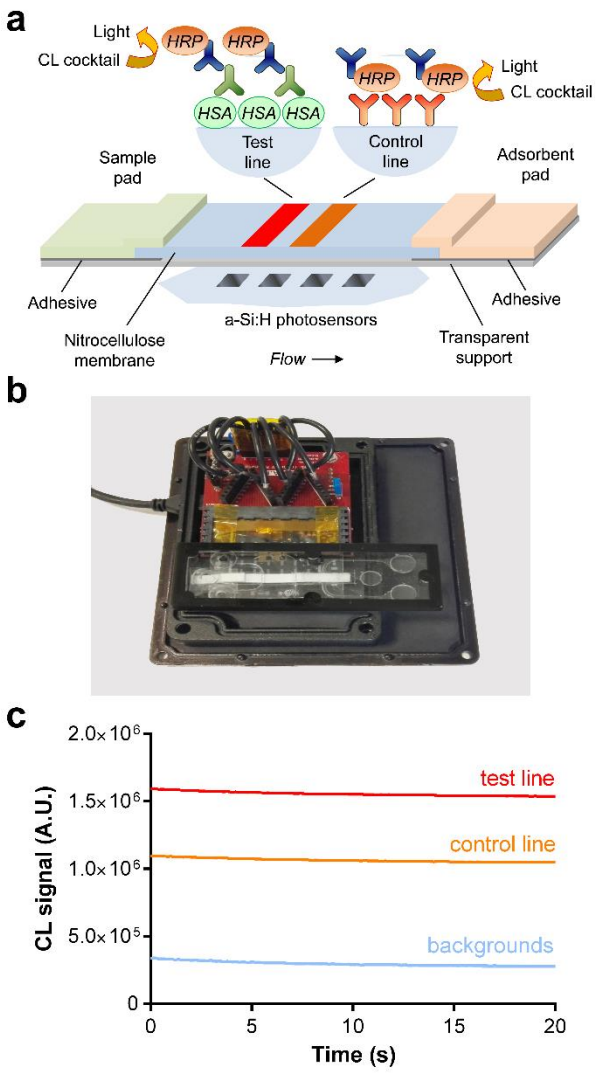

Figure 3

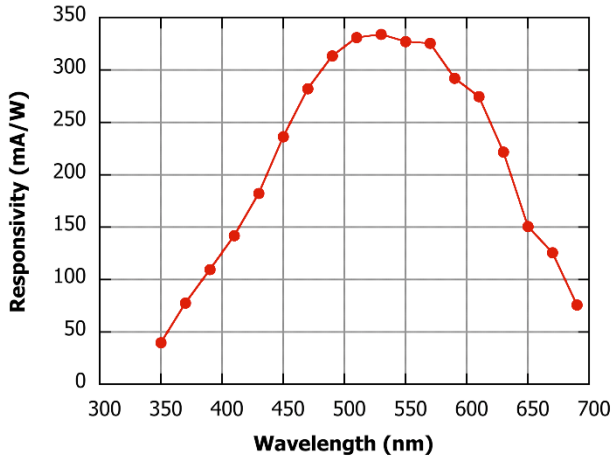

Figure 4

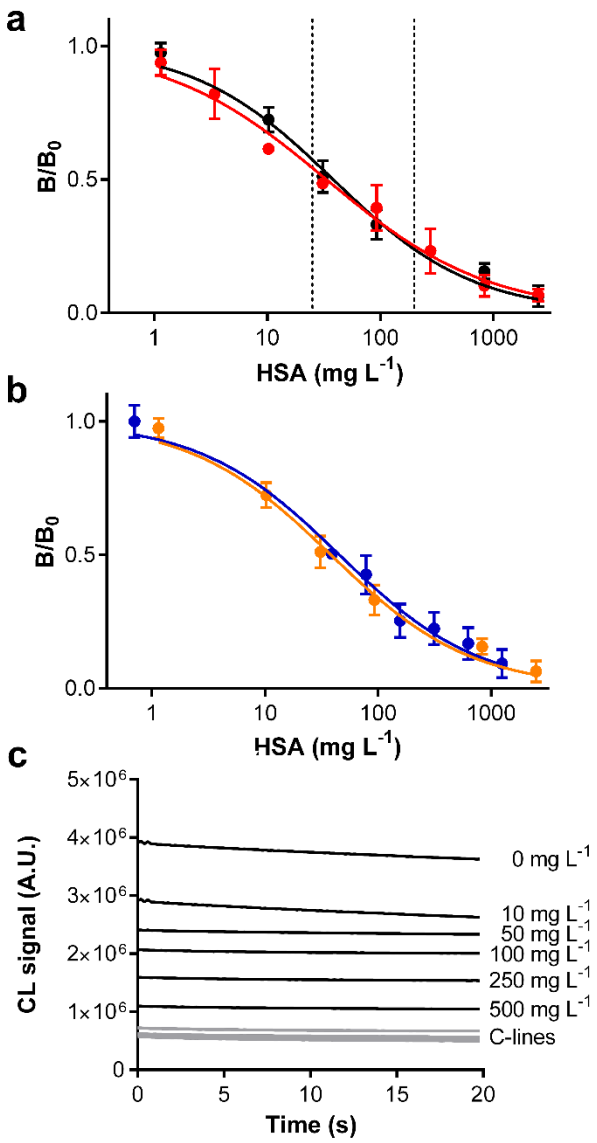

Figure 5

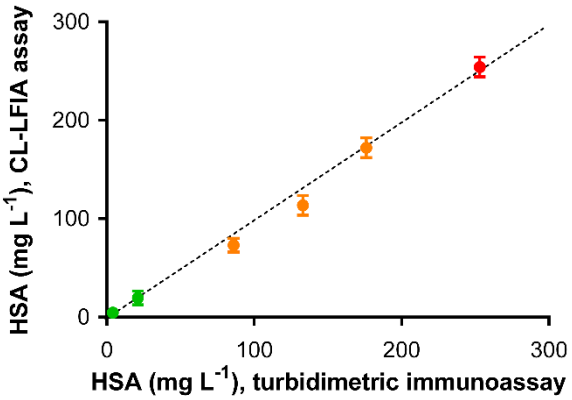

Figure 6